Isoscalar Giant Dipole Resonance of Tin Isotopes

112,114,116,118,120,122,124Sn Using HF- BCS and QRPA Approximations

Wafaa A. Mansour[*], Ali H. Taqi

Department of Physics, College of Science, University of Kirkuk, Kirkuk, Iraq.
*Corresponding author : ✉ wafawahk@gmail.com

CrossMark

Abstract

The isoscalar giant dipole resonance (ISGDR) of the even-even Tin isotopes 112,114,116,118,120,122,124Sn has been investigated by using fully self-consistent quasiparticle random phase approximation (QRPA) based on Bardeen Cooper Schriffer-Hartree Fock (HF-BCS). We depend on five sets of Skyrme-type interactions (T5, SKM, SLY4, SGII, and SKX) with varying effective mass m^*/m and nuclear matter incompressibility coefficient K_{NM}. Furthermore, the calculations incorporate the effects of several pairing force types, such as volume, surface, and mixed. The calculated strength distributions, scaled energies E_s, constrained energies E_{con}, and centroid energies E_{cen} of the ISGDR for the investigated isotopes are compared with the available experimental data. Analysis is done on the relationships between K_{NM} and m^*/m, and the estimated properties.

1. Introduction:

The goal of theoretical and experimental researches in the field of nuclear physics was to develop a method that could be utilized to precisely and universally describe nuclear structure, as our current understanding of the structure is still lacking and insufficient. A many-body problem exists in the theoretical nuclear structure. It is impossible to compute the complete model space since the quantum many-body problem is a computational problem for which there isn't yet a fully suitable answer. The Mean-field models with self-consistent properties are suitable to describe the nuclear structure [1] and [2].

In nuclei, the collective modes study was the subject of extensive theoretical and experimental studies during many contracts [3] and [4], where the Giant Resonances (GR) are an example of collective modes in atomic nuclei. Giant resonances (GR) are the high-frequency collective excitations of finite nuclear systems [5]. Understanding the strength distributions of these GR in a wide range of atomic nuclei yields valuable information about the finite nuclei as well as about the bulk nuclear matter [6] and [7]. The isoscalar dipole mode is the "compressional mode" and is especially important be-

cause its resonance energy is directly related to the nuclear incompressibility [8].

For closed-shell and closed sub-shell nuclei, the Hartree-Fock (HF) theory has previously proven to be an efficient technique for characterizing the properties of ground states. Microscopic models based on the self-consistent HF and Random Phase Approximation (RPA) is appropriate for representing collective modes like ISGDR [9]. In open-shell nuclei, nuclear pairing's outcome is crucial. A simple description of the ground-state pairing is provided by the HF+Bardeen-Cooper-Schriffer (BCS).

Quasiparticle Random Phase Approximation (QRPA) is an enhanced RPA model based on the HF- BCS model that accounts for the pairing effect, which is assumed to be significant for open-shell nuclei. This allows us to analyze the nuclear structure of the complete nuclear chart. Furthermore, relativistic methods such as Relativistic Continuum Random Phase Approximation (RCRPA) [10] and Relativistic Quasi Particle Random Phase Approximation (RQRPA) [11] exist.

Understanding the structure of nuclei and predicting the exotic properties of nuclei far from stability valley can both be done by studying the nuclear collective excitations. For modeling these collective excitations in open-shell nuclei with stable mean-field solutions, the QRPA is a widely used technique [12] and [13]. The nuclear compressional modes, in particular the ISGDR, which provide the best method for determining the nuclear incompressibility, are significant nuclear collective excitations [14] and [15]. Nuclear collective excitations and nuclear incompressibility have lately been studied using both nonrelativistic RPA [16], [17], [18] and [19] and relativistic RPA or QRPA [20] and [21].

Inelastic scattering of deuterons or alpha particles to modest forward angles is the main experimental technique for investigating the ISGDR. The methods created and put into use in the RCNP at Osaka University, Texas AM University Cyclotron Institute, and KVI in Groningen have made it possible to gather in-depth data on the ISGDR gross structure in a range of nuclear systems, see review [22]. The experimental data of ISGDR for Sn isotopes can be obtained in previously published papers [23], [24] and [25].

The present study aims to investigates theoretically the isoscalar giant Dipole resonance (ISGDR) in the isotopes of ^{112,114,116,118,120,122,124}Sn using the Skyrme QRPA method and the HF-Bardeen-Cooper-Schrieffer (HF-BCS) theory. Five sets of Skyrme parameters T5 [26], SKM [27], SLY4 [28], SGII [29], and SKX [30] of different values of nuclear matter incompressibility K_{NM} and effective mass m^*/m, as well as, of different types of pairing forces (i.e., volume, surface, and mixed) to be examined.

2. Theoretical Formulations:

The nuclear properties of both ground states and excited states can be described by the Skyrme effective interaction

[31], [32], [33], [34] and [35],

$$
\begin{aligned}
V(r_1-r_2) =& t_0(1+x_0P_\sigma)\delta(r_1-r_2) + \frac{t_1}{2}(1+x_1P_{12}^\alpha)[\overleftarrow{k}_{12}^2 \\
& \delta(r_1-r_2) + \delta(r_1-r_2)\overrightarrow{k}_{12}^2] + t_2(1+x_2P_{12}^\alpha)\overleftarrow{k}_{12} \\
& \delta(r_1-r_2)\overrightarrow{k}_{12} + \frac{t_3}{6}(1+x_3P_{12}^\alpha)\rho^\alpha(R)\delta(r_1-r_2) \\
& + iW_0\overleftarrow{k}_{12}\delta(r_1-r_2)(\overrightarrow{\sigma}_1+\overrightarrow{\sigma}_2)\overrightarrow{k}_{12}
\end{aligned}
\tag{1}
$$

where $\overleftarrow{k}_{12} = -\frac{i(\overleftarrow{\nabla}_1-\overleftarrow{\nabla}_2)}{2}$, $\overrightarrow{k}_{12} = -\frac{i(\overleftarrow{\nabla}_1-\overleftarrow{\nabla}_2)}{2}$, while $\overrightarrow{\sigma}_i$ and P_{12}^α is the is the Pauli spin and spin-exchange operators, respectively.

The total energy E of HF equations based on Skyrme's interaction as a result of single-particle functions φ can be calculated using the variational approach $<\delta\varphi|H(r)|\varphi> = 0$.

The HF equations are coupled to the standard BCS equations, that in spherical symmetry the particle number n and gap equation Δ_a read as,

$$
n = \sum_a (2j_a+1)v_a^2, \quad and \quad \Delta_a = -\sum_b \frac{\Delta_b}{2E_b}V_{a\bar{a}b\bar{b}}
\tag{2}
$$

where the tilde designates the time-reversal state, and E and v are the typical quasi-particle energies and BCS amplitudes, respectively. the matrix elements $V_{a\bar{a}b\bar{b}}$ are calculated using a zero-range, density-dependent pairing force of the type,

$$
V_{pair}(\mathbf{r_2},\mathbf{r_2}) = V_0\left[1+\eta\left(\frac{\rho(\frac{\mathbf{r_1}+\mathbf{r_2}}{2})}{\rho_0}\right)\delta(\mathbf{r_1}-\mathbf{r_2})\right]
\tag{3}
$$

where the nuclear saturation density $\rho_0 = 0.16$ fm^{-1}. For the volume, mixed, or surface pairing interactions, the value of V_0 is regarded as $0, 0.5$, or 1, respectively. Table 1 contains the values of V_0 that we have determined by fitting the experimental data of the mean neutron gap of ^{120}Sn ($\Delta n = 1.321$ MeV). Due to the closed proton shells associated with $Z = 50$ in these nuclei, there is only neutron pairing.

The total HF-BCS energy can be calculated directly from the force, or energy functional,

$$
E = E_{KE} + E_{Skyrme} + E_{Coul} + E_{Pair}
\tag{4}
$$

Where $E_{KE}, E_{Skyrme}, E_{Coul}$ and E_{Pair} are the Kinetic, Skyrme, Coulomb and Pair contributions to the energy, respectively.

First, a solution is found for the Skyrme HF-BCS equation for the ground state in coordinate space. The radial mesh used to solve the equations has a coverage area of up to 18 fm and a mesh size of 0.1 fm. This radial mesh is sufficiently large to generate stable results for all the nuclei under investigation.

In closed shell and sub-shell nuclei, collective excitations are usually described by means of the so-called RPA with

Table 1. Our estimated pairing strength V_0 to reproduce the empirical pairing gaps of ^{120}Sn (Δ_n = 1.321 MeV) for Volume (V), surface (S), and mixed (M) types of pairing interactions.

	T5			SKM			SLY4			SGII			SKX		
	Pairing strength V_0 (MeV fm^3) of types: Volume (V), Surface (S) and Mixed (M)														
	V	S	M	V	S	M	V	S	M	V	S	M	V	S	M
^{112}Sn	227.0	689.0	343.0	231.5	741.5	355.0	269.0	792.0	404.0	304.0	899.0	456.0	200.5	731.0	315.0
^{114}Sn	237.5	716.0	358.0	226.5	728.0	347.5	272.0	799.0	407.0	316.5	945.0	476.0	201.3	733.5	317.5
^{116}Sn	250.0	751.5	376.5	224.0	725.0	344.0	277.0	815.5	414.5	932.5	473.5	201.5	738.5	317.5	
^{118}Sn	259.5	775.5	390.5	225.0	733.0	345.0	282.0	832.5	423.5	308.5	907.5	462.0	200.0	736.0	316.0
^{120}Sn	273.0	807.0	412.0	228.0	750.5	351.5	286.5	855.0	430.5	305.0	897.0	456.0	203.0	750.0	320.0
^{122}Sn	274.5	823.0	413.5	234.0	782.5	362.0	290.5	874.0	438.5	303.5	898.0	456.0	207.0	770.0	328.0
^{124}Sn	276.0	816.0	415.0	245.0	830.0	381.0	298.5	908.0	450.1	293.0	861.5	439.5	215.4	809.0	340.8

Table 2. Shows the effective mass m*/m, and the nuclear matter incompressibility coefficient K_{NM} of the following Skyrme-type interaction.

Type	m*/m	K_{NM} (MeV)
T5	1.0	201.7
SKM	0.79	216.7
SLY4	0.69	229.9
SGII	0.79	269
SKX	0.99	270

stable mean-field solutions. The particle-particle and particle-hole channels are included in the extension of QRPA to open-shell nuclei. In order to solve the self-consistent QRPA, the Skyrme HF-BCS equations must be solved in order to obtain the ground state characteristics. Based on the $HF + BCS$ ground state, the $\nu - th$ excited state E_x^ν can be calculated using the QRPA. The compact form of QRPA equations can be written as follows: [36] and [37],

$$\begin{pmatrix} A_{ab,cd} & B_{ab,cd} \\ -B_{ab,cd}^* & -A_{ab,cd}^* \end{pmatrix} \begin{pmatrix} X_{cd}^\nu \\ Y_{cd}^\nu \end{pmatrix} = E_x^\nu \begin{pmatrix} X_{ab}^\nu \\ Y_{ab}^\nu \end{pmatrix}, \quad (5)$$

where X^ν and Y^ν are the corresponding amplitudes. The matrices A and B on the HF-BCS two-quasiparticle bases have the form,

$$\begin{aligned} A_{ab,cd} = &(1+\delta_{ab})^{-\frac{1}{2}}(1+\delta_{cd})^{-\frac{1}{2}}[(E_a+E_b)\delta_{ac}\delta_{bd}+(u_au_bu_c \\ &u_d+v_av_bv_cv_d)G(abcd;J)+(u_av_bu_cv_d+v_au_bv_cu_d) \\ &F(abcd;J)-(-1)^{j_c+j_d-J'}(u_av_bv_cu_d+v_au_bu_cv_d) \\ &F(abdc;J)], \end{aligned}$$

$$(6)$$

$$\begin{aligned} B_{ab,cd} = &(1+\delta_{ab})^{-\frac{1}{2}}(1+\delta_{cd})^{-\frac{1}{2}}[-(u_au_bv_cv_d+v_av_bu_cu_d) \\ &G(abdc;J)-(-1)^{j_c+j_d-J'}(u_av_bu_cv_d+v_au_bv_cu_d) \\ &F(abcd;J)+(-1)^{j_a+j_b+j_c+j_d-J-J'}(u_av_bv_cu_d+ \\ &v_au_bu_cv_d)F(abcd;J)], \end{aligned}$$

$$(7)$$

with

$$G(abcd;J) = \sum_{m_am_bm_cm_d} <j_am_aj_bm_b|JM><j_cm_cj_dm_d|J'M'> \\ \times V_{ab,cd}^{pp}$$

$$(8)$$

$$F(abcd;J) = \sum_{m_am_bm_cm_d} <j_am_aj_bm_b|JM><j_cm_cj_dm_d|J'M'> \\ \times V_{ab,cd}^{ph}$$

$$(9)$$

$V_{ab,cd}^{pp}$ and $V_{ab,cd}^{ph}$ are matrix elements of particle-particle (pp) and particle-hole (ph) effective interaction, respectively. The ph matrix elements $V_{ab,cd}^{ph}$ is defined as [16],

$$V_{ab,cd}^{ph} = -\sum_{J'}(2J'+1)\begin{Bmatrix} j_a & j_d & J' \\ j_c & j_b & j \end{Bmatrix}V_{ad,cb}^{pp} \quad (10)$$

The moments can be obtained using the following equation,

$$m_k = \int E^k S(E) dE \quad (11)$$

where S(E) is the strength function [14],

$$S(E) = \sum_\nu |<\nu|\hat{F}_J|O>|^2 \rho_\Gamma(E-E_\nu) \quad (12)$$

associated with the monopole operator where the Lorentzian function is defined as in the following,

$$\rho_\Gamma(E - E_\nu) = \frac{\Gamma}{2\pi} \frac{1}{(E - E_\nu)^2 + (\frac{\Gamma}{2})^2} \tag{13}$$

with Γ is the smearing parameter.

Three ratios can be calculated using these different sum rules: The centroid energy, $E_{cen} = \frac{m_1}{m_0}$, the constrained energy $E_{con} = \sqrt{m_1/m_{-1}}$, and the scaling energy $E_s = \sqrt{m_3/m_1}$, (where m_1 is the energy-weighted sum rule (EWSR), m_{-1} is the inverse energy-weighted sum rule, and m_3 is the cubic energy-weighted sum rule) [38].

3. Results and Discussion:

To study the isoscalar giant Dipole resonance (ISGDR) in the isotopes of ^{112,114,116,118,120,122,124}Sn, the static HF-BCS equations were solved by using the Numerov method with the radial mesh size $h = 0.1$ fm within a model space based on five Skyrme interaction sets, namely: T5 [26], SKM [27], SLY4 [28], SGII [29], and SKX [30] of the effective mass m^*/m, and the nuclear matter incompressibility coefficient K_{NM} are presented in Table 2. Different types of pairing forces (i.e., volume, surface, and mixed) are used. The diagonalization of QRPA matrix has been done in the selected model space using the code Skyrme_qrpa, which is modified version of the skyrme_rpa code [16].

In Figure 1, the calculated ISGDR strength distributions for the examined ^{112,114,116,118,120,122,124}Sn isotopes with the five Skyrme sets (T5, SKM, SLY4, SGII, and SKX) as a result of volume pairing force (dark green line) are compared with the available experimental data from Refs. [23] and [24] (black error bars).

A peak at about $25 - 27$ MeV is produced by the five Skyrme interactions. The peak energy depends on the type of interaction, where the lowest was for T5, followed by the SKM, SLY4, and SGII results, which are in the middle, and the SKX result is remarkably similar to the experimental data, which, in accordance with the associated incompressibility values, is found at the maximum energy.

The calculated ISGDR centroid energy E_{cen}, constrained energy E_{con}, and the scaling energy E_s are presented in Table 3 isotopes by combining the mixed pairing interaction with the parameter sets for T5, SKM, SLY4, SGII, and SKX. The experimental data were obtained from Ref. [25]. The values between parentheses represent the discrepancy between theoretical values and experimental data. All interaction results underestimated the data, except using SKX. The peak energies for the examined isotopes of Sn are better with the interaction SKX, which closely fits the experimental data. In Figure 2, the calculated ISGDR centroid energy E_{cen}, constrained energy E_{con}, and the scaling energy E_s, are plotted vs. mass numbers A of the investigated ^{112,114,116,118,120,122,124}Sn isotopes and

compared with the available experimental data of Ref. [25], the forces T5, SKM, SLY4, SGII, and SKX are adopted for various types of pairing (volume, surface, and mixed).

However, it is also evident that the anticipated centroid energies produced using the SGII interaction do not correspond with the experimental data, also, the T5, SKM, and SLY4 findings underestimated the experimental data, even when pairing effects were taken into consideration. The predictions using SKX are significantly better. As a result, there is still some mystery surrounding the difference between the values of the nuclear incompressibility obtained from the Sn data. However, pairing effects must be taken into account to lessen the difference between the values of the nuclear incompressibility extracted from Sn data.

In Figures 3 and 4, the K_{NM} incompressibility coefficient and the effective mass m^*/m are displayed against the computed centroid energies E_{cen}, restricted energy E_{con}, and scaling energy E_s, of the ISGDR. The dashed lines define the experimental region obtained from the experiments [25]. Overall, we see a correlation between the E_{cen} and K_{NM} and m^*/m for various types of pairing (volume, surface, and mixed).

For the case of the E_{cen} of ^{114,116,118,120,124}Sn, all Skyrme-types interactions underestimate the experimental data excluding SKX as shown in Figures 3 and 4, associated with a value of ($K_{NM} = 201.7 - 269$ MeV, $m^*/m = 0.69 - 1$) that reproduced the experimental result for E_{cen}. The E_{cen} of ^{112}Sn agree with the experimental data using the SGII and SKX Skyrme-types, the E_{cen} of ^{122}Sn with all types of Skyrme interaction are mostly smaller than the experimental result.

The E_{con} of Sn isotopes understudy with all types of Skyrme interaction are mostly smaller than the experimental result, except ^{112,114,116}Sn with the Skyrme interaction (SKX) is in agreement with the experimental data, associated with a value of ($K_{NM} = 270$ MeV, $m^*/m = 0.99$).

The E_s values for ^{114,118,120,122}Sn are in agreement with the experimental data using the SKM and SLY4 Skyrme interaction, with a value of ($K_{NM} = 216.7, 229.9$ MeV, $m^*/m = 0.79, 0.69$), while its values for ^{112,114,116}Sn are in agreement with the experimental data using the T5 Skyrme interaction with ($K_{NM} = 201.7$ MeV, $m^*/m = 1$), The other interactions are not agreed with the experimental data.
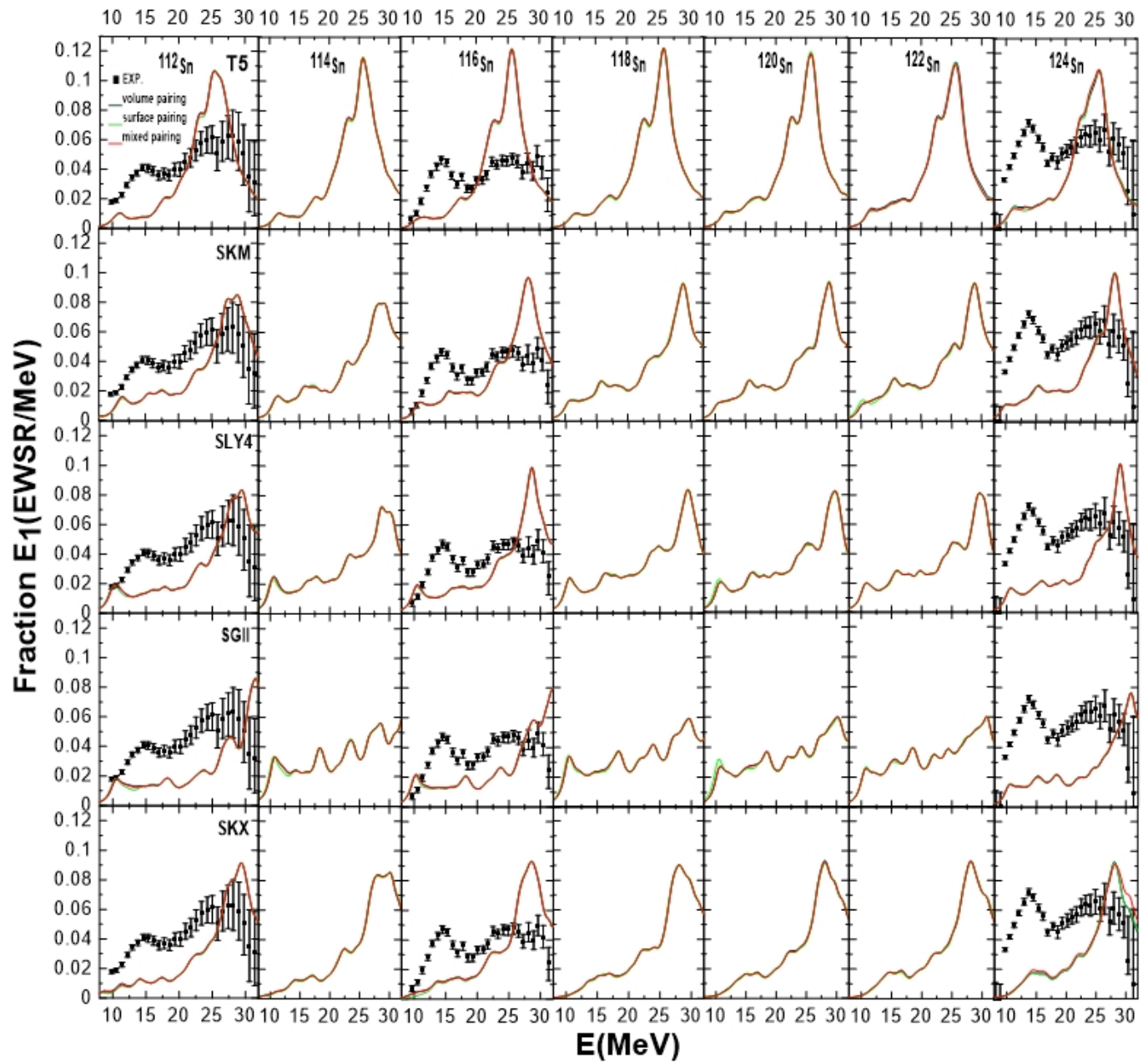
Figure 1. The experimental data (black-error bars) [23] and [24] for the examined Sn isotopes are contrasted with our calculated Fraction E1 (EWSR/MeV) of ISGDR. The Skyrme forces T5, SKM, SLY4, SGII, and SKX are used for the different pairing types: volume (dashed-blue line, surface (dashed-green line), and mixed (dashed-red line).
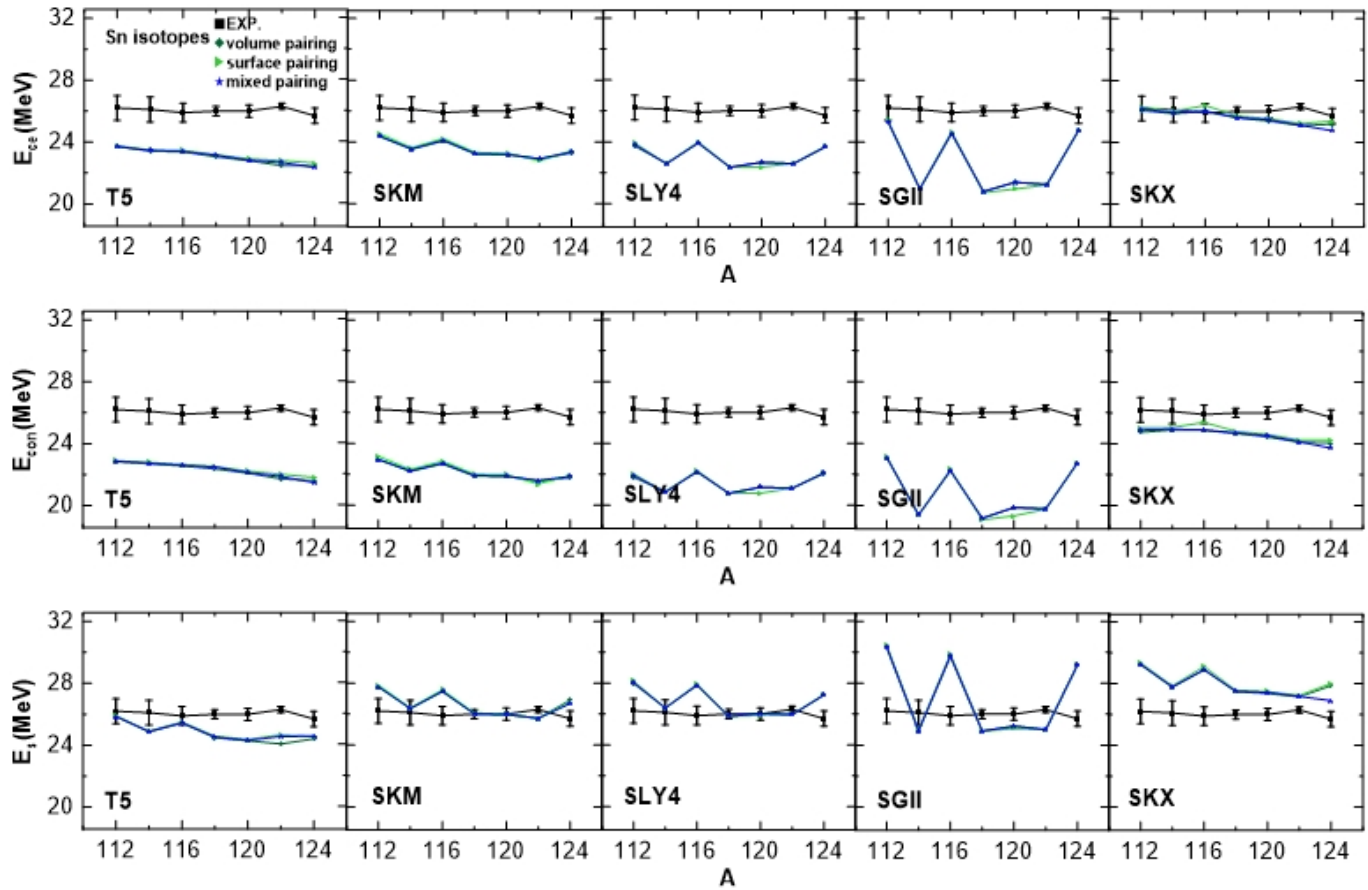
Figure 2. The calculated ISGDR (colored-solid lines) centroid energy E_{cen}, constrained energy E_{con}, and scaling energy E_s are compared with the experimental data [25]for the investigated Sn isotopes. Different pairing types: volume (dark green-diamond symbolled line), surface (green-triangle symbolled line, and mixed (blue-star symbolled line) are applied using the forces T5, SKM, SLY4, SGII, and SKX.
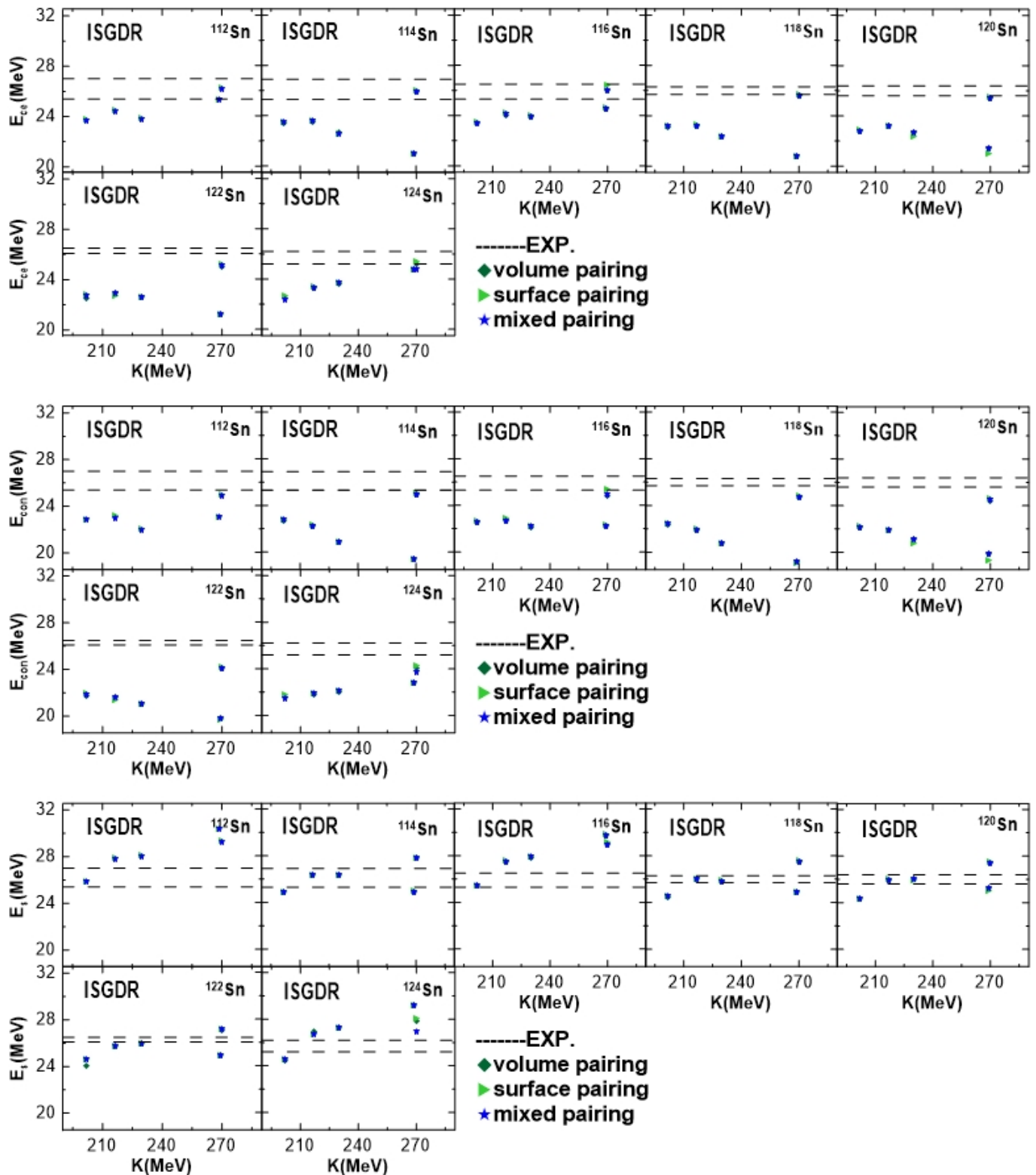
Figure 3. The calculated ISGDR centroid energy E_{cen}, constrained energy E_{con}, and scaling energy E_s vs. nuclear matter incompressibility coefficient K_{NM} for the investigated Sn isotopes are plotted by combining the mixed pairing interaction: volume (dark green-diamond symbolled line), surface (green-triangle symbolled line, and mixed (blue-star symbolled line) with the parameter sets for T5, SKM, SLY4, SGII, and SKX, and compared with the experimental data (Regions between the dashed black lines) [25].
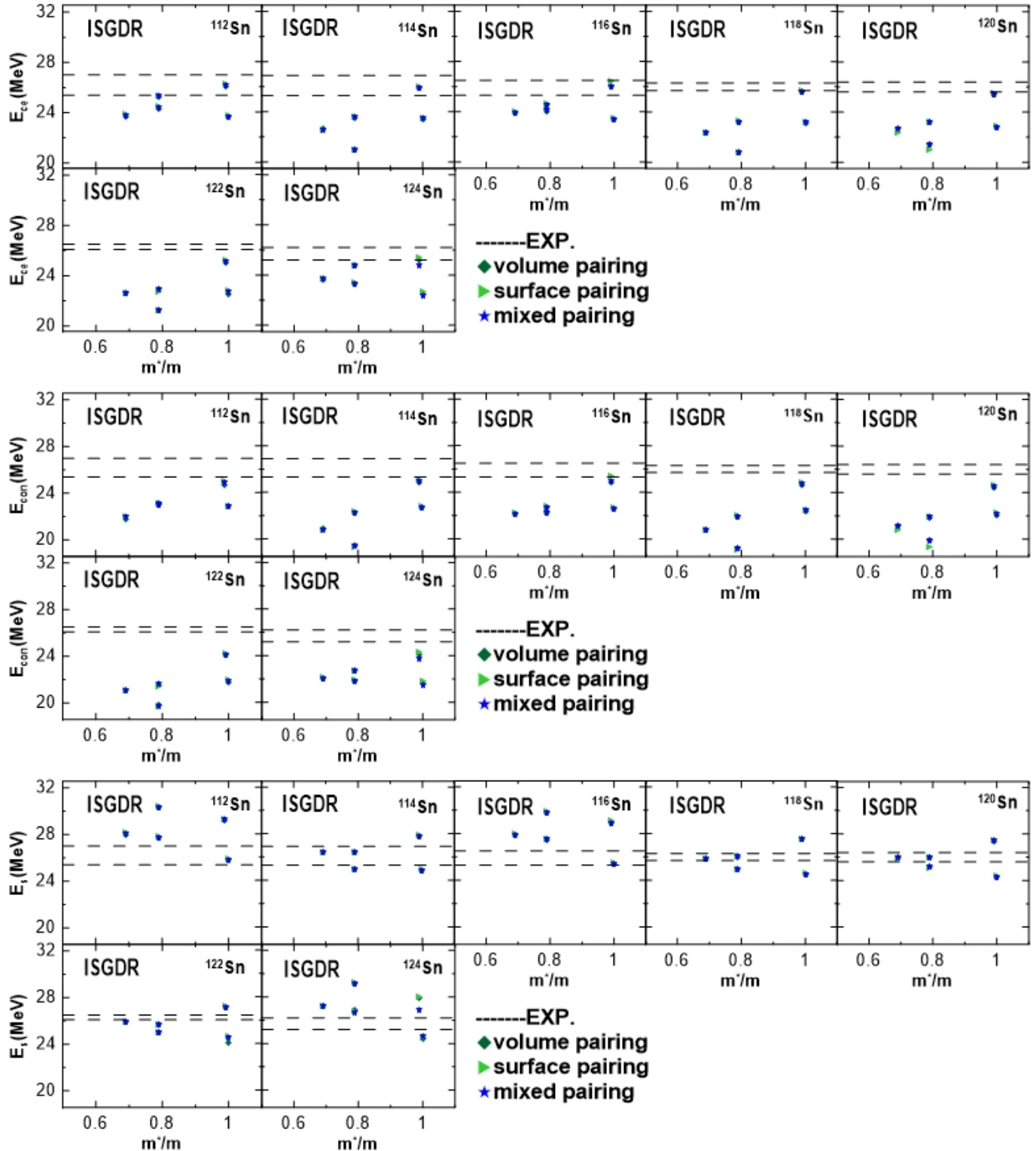
Figure 4. The calculated ISGDR centroid energy E_{cen}, constrained energy E_{con}, and scaling energy E_s vs. nuclear matter effective mass m^*/m are compared with the experimental data (Regions between the dashed black lines) [25] for the investigated Sn isotopes. The forces T5, SKM, SLY4, SGII, and SKX are adopted along m^*/m for various types of pairing: volume (dark green-diamond symbolled line), surface (green-triangle symbolled line, and mixed (blue-star symbolled line.

Table 3. The calculated E_{cen}, E_{con} and E_s for ISGDR in the investigated Sn isotopes by combining the mixed pairing interaction with the parameter sets for T5, SKM, SLY4, SGII, and SKX. The experimental information was collected from reference [25]. The difference between theoretical values and experimental data is shown by the quantities in parentheses.

	Exp.	T5	SKM	SLY4	SGII	SKX
			E_{cen} (MeV)			
^{112}Sn	26.2±0.8	23.75 (2.45)	24.54 (1.66)	23.93 (2.27)	25.38 (0.82)	26.29(-0.09)
^{114}Sn	26.1±0.8	23.49 (2.61)	23.62 (2.48)	22.58 (3.52)	20.97 (5.13)	25.99 (0.11)
^{116}Sn	25.9±0.6	23.46 (2.44)	24.22 (1.68)	24.00 (1.9)	24.66 (1.24)	26.39(-0.49)
^{118}Sn	26±0.3	23.18 (2.82)	23.31 (2.69)	22.36 (3.64)	20.73 (5.27)	25.70 (0.3)
^{120}Sn	26±0.4	22.92 (3.08)	23.26 (2.74)	22.38 (3.62)	20.96 (5.04)	25.53 (0.47)
^{122}Sn	26.3±0.2	22.80 (3.50)	22.78 (3.52)	22.59 (3.71)	21.23 (5.07)	25.21 (1.09)
^{124}Sn	25.7±0.5	22.64 (3.06)	23.42 (2.28)	23.71 (1.99)	24.76 (0.94)	25.37 (0.33)
			E_{con} (MeV)			
^{112}Sn	26.2±0.8	22.89 (3.31)	23.17 (3.03)	22.04 (4.16)	23.12 (3.08)	25.06 (1.14)
^{114}Sn	26.1±0.8	22.79 (3.31)	22.31 (3.79)	20.83 (5.27)	19.36 (6.74)	25.07 (1.03)
^{116}Sn	25.9±0.6	22.66 (3.24)	22.85 (3.05)	22.24 (3.66)	22.32 (3.58)	25.38 (0.52)
^{118}Sn	26±0.3	22.52 (3.48)	22.01 (3.99)	20.77 (5.23)	19.07 (6.93)	24.81 (1.19)
^{120}Sn	26±0.4	22.23 (3.77)	21.96 (4.04)	20.78 (5.22)	19.33 (6.67)	24.60 (1.4)
^{122}Sn	26.3±0.2	22.02 (4.28)	21.38 (4.92)	21.10 (5.2)	19.76 (6.54)	24.25 (2.05)
^{124}Sn	25.7±0.5	21.82 (3.88)	21.93 (3.77)	22.16 (3.54)	22.76 (2.94)	24.27 (1.43)
			E_s (MeV)			
^{112}Sn	26.2±0.8	25.89 (0.31)	27.89 (-1.69)	28.13 (-1.93)	30.41 (-4.21)	29.35(-3.15)
^{114}Sn	26.1±0.8	24.90 (1.2)	26.39 (-0.29)	26.39 (-0.29)	24.96 (1.14)	27.86(-1.76)
^{116}Sn	25.9±0.6	25.50 (0.4)	27.57 (-1.67)	27.94 (-2.04)	29.87 (-3.97)	29.11(-3.21)
^{118}Sn	26±0.3	24.58 (1.42)	26.07 (-0.07)	25.86 (0.14)	24.91 (1.09)	27.57(-1.57)
^{120}Sn	26±0.4	24.38 (1.62)	26.01 (-0.01)	25.92 (0.079)	25.06 (0.94)	27.48(-1.48)
^{122}Sn	26.3±0.2	24.68 (1.62)	25.72 (0.58)	25.97 (0.33)	24.99 (1.31)	27.24(-0.94)
^{124}Sn	25.7±0.5	24.59 (1.11)	26.76 (-1.06)	27.27 (-1.57)	29.21 (-3.51)	28.01(-2.31)

4. Conclusions:

A significant description of the collective low-lying IS-GDR is done. The peak high, widths, and (smooth) profiles of strength of the examined ^{112}Sn, ^{116}Sn, ^{124}Sn isotope with SGII, SKX agree with the data. The E_{cen}, E_{con}, E_s values that are in agreement with experimental data are those that drop as A increases and those that use interactions of K_{NM} between 269 and 270 MeV. The current investigation reveals that a correlation between the calculated energies (E_{cen}, E_{con}, and E_s) and the nuclear incompressibility constant K_{NM}, but there is an effect of the effective mass m^*/m. We concluded that the gap between the nuclear incompressibility values obtained from the Sn data is reduced with the use of pairing, and the surface pairing generates results that are essentially closer to the experimental data. We have also found that the change of the ISGDR, energies by pairing correlations in $^{112-124}$Sn is quite small. Pairing helps in reducing the discrepancy between the values of the nuclear incompressibility extracted from Sn data. A small discrepancy of about 5% in K_{NM} between the conclusions drawn from Sn data remains and may deserve further investigation. Since the size of this discrepancy depends on the pairing force and the model to treat its effects, one should better analyze whether we can constrain the attractive particle-particle matrix elements that appear in the QRPA calculations.

Funding: None.

Data Availability Statement: All of the data supporting the findings of the presented study are available from corresponding author on request.

Declarations:
Conflict of interest: The authors declare that they have no conflict of interest.

Ethical approval: The manuscript has not been published or submitted to another journal, nor is it under review.

References

[1] P. Ring and P. Schuck. The nuclear many-body problem. *Journal of travel medicine*, 36(7): 70, 1983, doi:10.1063/1.2915762.

[2] J.-P. Blaizot and G. Ripka. *Quantum Theory of Finite Systems*. MIT press Cambridge, MA, 1986.

[3] A. Bohr and B. R. Mottelson. *Nuclear Structure, Vol. II: Nuclear Deformation*. London: Imperial College Press and World Scientific Publishing Co. Pte. Ltd, 1998.

[4] S. Shlomo, V. M. Kolomietz, and G. Colo. Deducing the nuclear matter incompressibility coefficient from data on isoscalar compression modes. *European Physical Journal*, 30: 23–30, 2006, doi:10.1140/epja/i2006-10100-3.

[5] F. E. Bertrand. Giant multipole resonances - perspectives after ten years. *Nuclear Physics A*, 354: 129, 1981, doi:10.1016/0375-9474(81)90596-0.

[6] M. N. Harakeh and A. van der Woude. *Giant Resonances Fundamental High-Frequency Modes of Nuclear Excitation*. Oxford University Press, New York, 2001, doi:10.1093/oso/9780198517337.003.0001.

[7] J. M. Lattimer and M. Prakash. Neutron star strcture and the equion of state. *The Astrophysical Journal*, 550: 426, 2001, doi:10.1086/319702.

[8] S. Stringari. Sum rules for compression modes. *Physics Letters B*, 108(4-5)(): 232–236, 1982, doi:10.1016/0370-2693(82)91182-0.

[9] Nguyen Van Giai. Self-consistent description of nuclear excitations. *Progress of Theoretical and Experimental Physics*, 330: 74–75, 1983, doi:10.1143/PTPS.74.330.

[10] D. Vretenar, T. Nikšić, and P. Ring. A microscopic estimate of the nuclear matter compressibility and symmetry energy in relativistic mean-field models. *Physical Review Journals*, 68: 024310, 2003, doi:10.48550/arXiv.nucl-th/0302070.

[11] Von Ioannis Daoutidis. *Relativistic Continuum Random Phase Approximation in Spherical Nuclei*. PhD thesis, Technical University of Munich, 2009, doi:10.48550/arXiv.1103.2332.

[12] P. Ring and P. Schuck. The nuclear many-body problem. *Physics Today*, 36(7): 70, 1983, doi:10.1063/1.2915762.

[13] D. J. Rowe. *Nuclear collective motion*. Methuen, London, 2010, doi:10.1142/6721.

[14] Gullala A. Mohammed and Ali H. Taqi. Isoscalar dipole response in ^{92}Mo and ^{100}Mo isotopes. *Momento Revista de Física*, 67: 101, 2023, doi:10.15446/mo.n67.107907.

[15] S. Shlomo, V. M. Kolomietz, , and G. Colo. Deducing the nuclear-matter incompressibility coefficient from data on isoscalar compression modes. *The European Physical Journal A*, 30: 23, 2006, doi:10.1140/epja/i2006-10100-3.

[16] G. Colo, L. Cao, N. Van Giai, and L. Capelli. Self-consistent rpa calculations with skyrme-type interactions: The skyrme_rpa program. *Computer Physics Communications*, 184(1):142–161, 2013, doi:10.1016/j.cpc.2012.07.016.

[17] Giampaolo Co'. Introducing the random phase approximation theory. *Universe 2023*, 9(3): 141, 2023, doi:10.3390/universe9030141.

[18] P. Schuck, D. S. Delion, J. Dukelsky, M. Jemai, E. Litvinova, G. Röpke, and M. Tohyama. Equation of motion method for strongly correlated fermi systems and extended rpa approaches. *Physics Reports*, 929: 1–84, 2021, doi: https://doi.org/10.1016/j.physrep.2021.06.001.

[19] V. Tselyaev. Spurious dipole mode in random-phase approximation and in models based on this approximation. *Physical Review C*, 106: 064327, 2022, doi: 10.1103/PhysRevC.106.064327.

[20] Shi Yao Chang, Zhi Heng Wang, Yi Fei Niu, and Wen Hui Long. Relativistic random-phase-approximation description of m1 excitations with the inclusion of mesons. *Physical Review C*, 105: 034330, 2022, doi: 10.1103/PhysRevC.105.034330.

[21] Amandeep Kaur, Esra Yüksel, and Nils Paar. Electric dipole transitions in the relativistic quasiparticle random phase approximation at finite temperature. *Research and practice in thrombosis and haemostasis*, 2023, doi: 10.1002/rth2.12372.

[22] Umesh Garg and Gianluca Colò. The compression-mode giant resonances and nuclear incompressibility. *Irish Journal of Medical Science*, 190(4): 1649–52, 2021, doi:10.1007/s11845-020-02485-z.

[23] Y.-W. Lui, D. H. Youngblood, Y. Tokimoto, H. L. Clark, and B. John. Giant resonances in ^{112}Sn and ^{124}Sn: Isotopic dependence of monopole resonance energies. *Physical Review C*, 70: 014307, 2004, doi:10.1103/PhysRevC.70.014307.

[24] D. H. Youngblood, Y.-W. Lui, H. L. Clark, Y. Tokimoto B. John, and X. Chen. Isoscalar e0e3strength in $^{116}Sn, ^{144}Sm, ^{154}Sm, and ^{208}Pb$. *Physical Review C*, 69: 034315, 2020, doi: 10.1103/PhysRevC.69.034315.

[25] T. Li, U. Garg, Y. Liu, R. Marks, B. K. Nayak, P. V. Madhusudhana Rao, M. Fujiwara, H. Hashimoto, K. Kawase, K. Nakanishi, S. Okumura, M. Yosoi, M. Itoh, M. Ichikawa, R. Matsuo, T. Terazono, M. Uchida, T. Kawabata, H. Akimuneand Y. Iwao, T. Murakami, H. Sakaguchi, S. Terashima, Y. Yasuda, J. Zenihiro, and M. N. Harakeh. Isoscalar giant resonances in the Sn nuclei and implications for the asymmetry term in the nuclear-matter incompressibility. *Physical Review C*, 81: 034309, 2010, doi: 10.1103/PhysRevC.81.034309.

[26] F. Tondeur, M. Brack, M. Farine, and J. M. Pearson. Static nuclear properties and the parametrisation of skyrme forces. *Nuclear Physics A*, 420: 297, 1984, doi:10.1016/0375-9474(84)90444-5.

[27] Anna Maria Saruis. Self-consistent hf-rpa description of electron and photon nuclear reactions with skyrme forces. *Physics Reports*, 235: 794–800, 1993, doi:10.1016/0370-1573(93)90123-U.

[28] J. Rikovska Stone, J. C. Miller, R. Koncewicz, P. D. Stevenson, and M. R. Strayer. Nuclear matter and neutron-star properties calculated with the skyrme interaction. *Physical Review C*, 68: 034324, 2003, doi:10.1103/PhysRevC.68.034324.

[29] Nguyen Van Giai and H. Sagawa. Spin-isospin and pairing properties of modified skyrme interactions. *Physics Letters*, 116(5): 379–382, 1981, doi:10.1016/0370-2693(81)90646-8.

[30] B. Alex Brown. New skyrme interaction for normal and exotic nuclei. *Physical Review C*, 58: 220, 1998, doi:10.1103/PhysRevC.58.220.

[31] J. R. Stone and P. G. Reinhard. The skyrme interaction in finite nuclei and nuclear matter. *Progress in Particle and Nuclear Physics*, 58(2): 587, 2007, doi:10.1016/j.ppnp.2006.07.001.

[32] Ali H. Taqi and Ghanim L. Alawi. Isoscalar giant resonance in ^{100,116,132}Sn isotopes using skyrme HF-RPA. *Nuclear Physics*, 983: 103, 2019, doi:10.1016/j.mrfmmm.2014.06.001.

[33] Ali H. Taqi and Mohamed S. Ali. Self-consistent hartree-fock RPA calculations in ^{208}Pb. *Indian Journal of Physics*, 92(1): 69, 2021, doi:10.1007/s12648-017-1073-4.

[34] Ali H. Taqi and E.G. Khider. Ground and transition properties of ^{40}Ca and ^{48}Ca nuclei. *Nuclear Physics and Atomic Energy*, 19: 326, 2018, doi:10.15407/jnpae2018.04.326.

[35] Shyma'a. H. Amin, A. Aziz Al-Rubaiee, and Ali H. Taqi. Effect of incompressibility and symmetry energy density on charge distribution and radii of closed-shell nuclei. *Kirkuk Journal of Science*, 17(3): 17, 2022, doi:10.32894/kujss.2022.135889.1073.

[36] J. Kvasil, V.O. Nesterenko, A. Repko, W. Kleinig, and P.-G. Reinhard. Deformation induced splitting of the isoscalar e0 giant resonance: Skyrme random-phase-approximation analysis. *The Journal of Infection in Developing Countries*, 94: 064302, 2016, doi:10.1103/PhysRevC.94.064302.

[37] K. Yoshida and T. Nakatsukasa. Shape evolution of giant resonances in nd and sm isotopes. *Physical Review C*, 88: 034309, 2013, doi:10.1103/PhysRevC.88.034309.

[38] S. Stringari. Sum rules for compression modes. *Physics Letters B*, 108: 232, 1982, doi:10.1016/0370-2693(82)91182-0.

الرين ثنائي القطب العملاق العددي لنظائر القصدير $^{112,114,116,118,120,122,124}Sn$ باستخدام تقريبات $HF - BCS$ و $QRPA$

وفاء احمد منصور * ، علي حسين تقي

قسم الفيزياء،كلية العلوم، جامعة كركوك، كركوك، العراق.

الباحث المسؤول *: $wafawahk@gmail.com$

الخلاصة

قمنا في هذا العمل بدراسة الرين ثنائي القطب العملاق العددي $ISGDR$ لنظائر القصدير الزوجية – $^{112,114,116,118,120,122,124}Sn$ باستخدام تقريب الطور العشوائي شبه الجسيمي المتسق تمامًا مع نفسه $QRPA$ والمستند على باردين كوبر شريفر – هارتري فوك $HF - BCS$. في هذا العمل تم الاعتماد على خمس مجموعات من التفاعلات من نوع $Skyrme$: $T5$ و SKM و $SLY4$ و $SGII$ و SKX والتي تمتلك قيم مختلفة من الكتلة الفعالة $effective\ mass\ m^*/m$ ومعامل عدم انضغاط المادة النووية $incompressibility\ coefficient\ K_{NM}$ اضافة الى ذلك، تضمنت الحسابات تأثيرات عدة أنواع من قوة الاقتران، مثل الحجم والسطح والمختلط. تمت مقارنة توزيعات القوة المحسوبة $strength\ distributions$ والطاقات المتدرجة $scaled\ energies\ E_s$ والطاقات المقيدة $constrained\ energies\ E_{con}$ وطاقات النقطه الوسطى $centroid\ energies\ E_{cen}$ لحالة $ISGDR$ للنظائر المدروسة مع البيانات التجريبية المتاحة. تم تحليل العلاقات بين K_{NM} و m^*/m مع الخصائص التي تم ايجادها.

الكلمات الدالة : توزيع القوة؛ الرين ثنائي القطب العملاق العددي $(ISGDR)$ ؛ قوة سكيرمي؛ هارتري – فوك – باردين – كوبر – شريفير $(HF - BCS)$ ؛ تقريب الطور العشوائي شبه الجسيمي $(QRPA)$.